J|A|C|S
ARTICLES
Published on Web 12/15/2006

# Well-Defined Surface Imido Amido Tantalum(V) Species from Ammonia and Silica-Supported Tantalum Hydrides

Priscilla Avenier,[†] Anne Lesage,[‡] Mostafa Taoufik,[†] Anne Baudouin,[†] Aimery De Mallmann,[†] Steven Fiddy,[§] Manon Vautier,[†] Laurent Veyre,[†] Jean-Marie Basset,*[,†] Lyndon Emsley,*[,‡] and Elsje Alessandra Quadrelli*[,†]

*Contribution from the Laboratoire de Chimie Organométallique de Surface, UMR-9986 CNRS-CPE, 43 Boulevard du 11 Novembre 1918, BP 2077 F, 69616 Villeurbanne Cedex, France, Laboratoire de Chimie, UMR-5182 CNRS-ENS Lyon, Ecole Normale Supérieure de Lyon, 69364 Lyon Cedex, France, and Synchrotron Radiation Department, Beam-line 7.1, CCLRC Daresbury Laboratory, Warrington WA4 4AD, U.K.*

Received September 15, 2006; E-mail: basset@cpe.fr; lyndon.emsley@ens-lyon.fr; quadrelli@cpe.fr

***Abstract:*** The MCM-41 supported hydrides [(≡SiO)$_2$TaH], **1a**, and [(≡SiO)$_2$TaH$_3$], **1b**, cleave N−H bonds of ammonia at room temperature to yield the well-defined imido amido surface complexes [(≡SiO)$_2$Ta(NH)(NH$_2$)], **2**, and **2·NH$_3$**. Additionally, the surface silanes [≡Si−H] that exist in close proximity to **1a** and **1b** also react with ammonia at room temperature to give the surface silylamido [≡Si−NH$_2$]. Such reaction is tantalum assisted: surface silanes were synthesized independently and in absence of tantalum by reaction of highly strained silica, SiO$_{2-1000}$, with SiH$_4$ and no reaction with ammonia was observed. Surface-supported complexes **2**, **2·NH$_3$**, and [≡Si−NH$_2$] have been characterized by, inter alia, solid-state NMR, IR, and EXAFS and independent synthesis of [≡Si−NH$_2$]. The NMR studies on the fully $^{15}$N-labeled samples have led to unambiguous discrimination between imido, amido, and amino resonances of **2***, **2*·$^{15}$NH$_3$**, and [≡Si−$^{15}$NH$_2$] through the combination of solid-state magic angle spinning (MAS), heteronuclear correlation (HETCOR), 2D proton double-quantum (DQ) single-quantum (SQ) correlation, and 2D proton triple-quantum (TQ) single-quantum (SQ) correlation spectra. The in situ IR monitoring of the reaction of **1a** and **1b** with regular NH$_3$ and $^{15}$NH$_3$, and after H/D exchange has yielded the determination of all the NH$_x$ vibration and deformation modes, with their respective H/D and $^{14}$N/$^{15}$N isotopic shifts. EXAFS study yielded the bond distances in **2** of 1.79(2) Å for Ta═N, 1.89(1) Å for Ta−O, and 1.98(2) Å for Ta−N.

## 1. Introduction

Ammonia would be a valuable reactant for N-functionalization of organic substrates,[1,2] but chemistry relative to the key-step of metal-mediated ammonia addition to organic substrates does not exist to any substantial extent.[2] This absence has been linked to the scarcity of reactions achieving ammonia transformation to metal−amido and −imido reactions, and is explained by the propensity of NH$_3$ to coordinate through the nitrogen lone-pair rather than by oxidative addition of the N−H bond.[1,2]

The vast majority of the synthetic routes to metal−imido and −amido complexes use highly activated inorganic precursors such amides or other strong bases.[3−7] There are so far only two well-characterized[8] examples of the direct use of ammonia to synthesize imido or amido complexes by oxidative addition: {(Me$_3$SiNCH$_2$CH$_2$)$_3$N}Ta$^{III}$(C$_2$H$_4$) and {($^t$Bu$_2$PCH$_2$CH$_2$)$_2$CH}-Ir$^I$(CH$_2$CHR), that yield, respectively, the imido Ta(V) complex {(Me$_3$SiNCH$_2$CH$_2$)$_3$N}Ta$^V$═NH[9] and the amido hydride Ir(III) complex [{($^t$Bu$_2$PCH$_2$CH$_2$)$_2$CH}Ir$^{III}$(NH$_2$)H].[2] Direct use of ammonia not occurring through oxidative addition offers only one further example: the two d$^0$ complexes Cp*$_2$MH$_2$ (M = Zr and Hf) react with ammonia, to afford Cp*$_2$M(H)(NH$_2$) and H$_2$ elimination,[10] presumably by protonolysis.[2]

We report herein the room-temperature addition of ammonia to silica- and MCM-41-supported siloxy tantalum hydrides[11] [(≡SiO)$_2$TaH], **1a**, and [(≡SiO)$_2$TaH$_3$], **1b**, and the character-

[†] Laboratoire de Chimie Organométallique de Surface, UMR-9986 CNRS-CPE.
[‡] Laboratoire de Chimie, UMR-5182 CNRS-ENS Lyon, Ecole Normale Supérieure de Lyon.
[§] Synchrotron Radiation Department, Beam-line 7.1, CCLRC Daresbury Laboratory.

(1) Braun, T. *Angew. Chem., Int. Ed.* **2005**, *44*, 5012−5014.
(2) Zhao, J.; Goldman, A. S.; Hartwig, J. F. *Science* **2005**, *307*, 1080−1082.
(3) Fryzuk, M. D.; Montgomery, C. D. *Coord. Chem. Rev.* **1998**, *95*, 1.
(4) Chao, Y. W.; Wexler, P. A.; Wigley, D. E. *Inorg. Chem.* **1990**, *29*, 4592−4594.
(5) Parkin, G.; van Asselt, A.; Leathy, D. J.; Whinnery, L.; Hua, N. G.; Quan, R. W.; Henling, L. M.; Schaefer, W. P.; Santarsiero, B. D.; Bercaw, J. E. *Inorg. Chem.* **1992**, *31*, 82−85.
(6) Fox, D. J.; Bergman, R. G. *Organometallics* **2004**, *23*, 1656−1670.
(7) (a) Schrock, R. R.; Murdzek, J. S.; Bazan, G. C.; Robbins, J.; DiMare, M.; O'Regan, M. *J. Am. Chem. Soc.* **1990**, *112*, 3875−3886. (b) Joslin, F. L.; Johnson, M. P.; Mague, J. T.; Roundhill, D. M. *Organometallics* **1991**, *10*, 2781−2794. (c) Conner, D.; Jayaprakash, K. N.; Cundari, T. R.; Gunnoe, T. B. *Organometallics* **2004**, *23*, 2724−2733.
(8) Some precedents of low-yield or partially characterized imido and amido complexes from ammonia also exist; for example see: (a) Parkin, G.; van Asselt, A.; Leathy, D. J.; Whinnery, L.; Hua, N. G.; Quan, R. W.; Henling, L. M.; Schaefer, W. P.; Santarsiero, B. D.; Bercaw, J. E. *Inorg. Chem.* **1992**, *31*, 82−85. (b) Casalnuovo, A. L.; Calabrese, J. C.; Milstein, D. *Inorg. Chem.* **1987**, *26*, 971−973. (c) Bryan, E. G.; Johnson, B. F. G.; Lewis, J. *J. Chem. Soc., Dalton. Trans.* **1977**, 1328.
(9) Freundlich, J. S.; Schrock, R. R.; Davis, W. M. *J. Am. Chem. Soc.* **1996**, *118*, 3643−3655.
(10) Hillhouse, G. L.; Bercaw, J. E. *J. Am. Chem. Soc.* **1984**, *106*, 5472−5478.


10.1021/ja0666809 CCC: $37.00 

ization of the resulting Ta(V) amido imido complex by IR, EXAFS, and advanced solid-state NMR techniques, including a novel proton triple-quantum (TQ) correlation experiment so far never applied in surface science. Additionally, we show how ammonia also achieves Si−H direct amination at room temperature to [≡Si−$NH_2$] by reaction with the surface silanes present in **1a** and **1b**, and how this reaction is tantalum-mediated. The observed surface reactivity will be discussed in terms of the elementary steps of molecular organometallic chemistry and surface-related properties.

## 2. Results and Discussion

**2.1. Characterization of the Surface Organometallic Species.** The surface Ta(V) amido imido complex [(≡$SiO)_2$Ta(═NH)($NH_2$)], **2**, is obtained quantitatively by reaction of ammonia at room temperature with MCM-41-supported siloxy tantalum hydrides[11] [(≡$SiO)_2$TaH], **1a**, and [(≡$SiO)_2$$TaH_3$], **1b**. Each surface tantalum of the starting hydrides **1a** and **1b** possesses one surface silane hydride, [≡SiH] (or less often [≡$SiH_2$]),[12] in its close vicinity. These surface silanes also react with ammonia at room temperature to yield surface silylamido species, [≡Si−$NH_2$]. Dihydrogen is released in the gas phase during the reaction (see reaction 1).

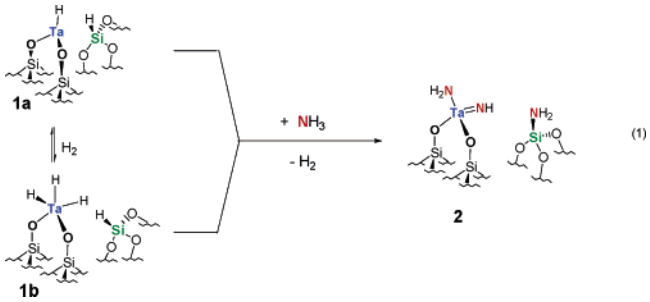


In the presence of excess ammonia, the surface complex **2** is in equilibrium with its ammonia adduct [(≡$SiO)_2$Ta(═NH)($NH_2$)($NH_3$)], **2·$NH_3$**. The relative final amounts of surface species **2**, **2·$NH_3$**, [≡Si−$NH_2$], and ammonia adsorbed on the silica surface critically depend on the reaction conditions. The typical experimental conditions that maximize the yield in [(≡$SiO)_2$Ta(═NH)($NH_2$)], **2**, are addition of a 4-fold excess of ammonia necessary to observe complete consumption of tantalum hydrides (monitored by in situ IR), 2-h reaction at room temperature followed by heating and evacuation of the gas phase at 80 °C for 4 h. The resulting solid contains 2.7 N/Ta, with respect to the expected 3.0 N/Ta for complete conversion to **2** and [≡Si−$NH_2$].[13]

The structure of the surface tantalum complex **2** has been characterized by solid-state NMR spectroscopy, IR spectroscopy,

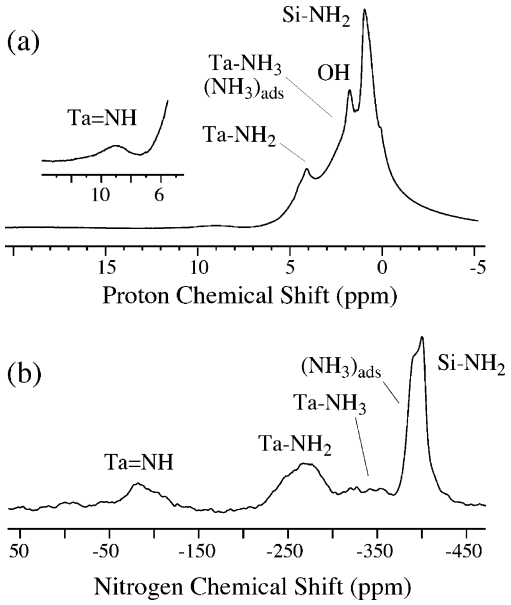


***Figure 1.*** One-dimensional $^1$H (a) and $^{15}$N (b) MAS NMR spectra of fully $^{15}$N-labeled complexes **2***, **2*·$^{15}$$NH_3$**, and [≡Si−$^{15}$$NH_2$]. The $^1$H spectrum was acquired using a single-pulse experiment with 64 scans and a recycle delay of 2 s. The $^{15}$N spectrum was obtained after cross polarization from protons (1 ms contact time) using an adiabatic ramped CP[55,56] (see Experimental Section for details). A total of 512 scans were acquired with a recycle delay of 2 s. During acquisition TPPM proton decoupling was applied at a RF field strength of $\omega_1 = 80$ kHz. For both spectra, the spinning frequency was $\omega_R = 12.5$ kHz.

and EXAFS. For the NMR studies, a fully $^{15}$N-enriched complex, **2*** (in equilibrium with **2*·$^{15}$$NH_3$**) was prepared from the reaction of the starting hydrides **1a** and **1b** with 4 equiv of fully labeled ammonia. Figure 1 shows the proton and nitrogen-15 one-dimensional (1D) magic angle spinning (MAS) spectra of the sample (Figure 1, a and b, respectively). The proton spectrum displays several unresolved resonances between −1 and 5 ppm as well as a weak broad peak at around 9 ppm. The nitrogen-15 cross polarization (CP) MAS spectrum shows three large resonances centered at about −87, −270, and −340 ppm plus two more intense and narrow peaks at −390 and −400 ppm. The assignment of the various resonances, indicated above the two spectra, was performed unambiguously through the combined analysis of two-dimensional $^{15}$N−$^1$H HETCOR (Figure 2a), proton double-quantum (Figure 2b), and proton triple-quantum (Figure 2c) spectra. In particular the resonances of the imido, amido, and amino resonances of complexes **2***, **2*·$^{15}$$NH_3$**, and [≡Si−$^{15}$$NH_2$] could be unequivocally identified and characterized as detailed below.

The 2D HETCOR spectrum, which yields correlations between spatially close $^1$H and $^{15}$N spins, displays five distinct correlations. The correlation centered at around (9 ppm, −90 ppm) is assigned to the tantalum imido moiety Ta(***NH***), in good agreement with solution NMR studies on imido molecular species which report proton and nitrogen-15 chemical shifts between 5 and 11 ppm, and between −100 and 50 ppm, respectively.[14] Note that this heteronuclear correlation is relatively weak and could not be observed in the absence of homonuclear decoupling during the indirect proton evolution period of the HETCOR experiment. The more intense correlation at (4.3 ppm, −270 ppm) is assigned to the tantalum amido

(11) Soignier, S.; Taoufik, M.; Le Roux, E.; Saggio, G.; Dablemont, C.; Baudouin, A.; Lefebvre, F.; De Mallmann, A.; Thivolle-Cazat, J.; Basset, J.-M.; Sunley, G.; Maunders, B. M. *Organometallics* **2006**, *25*, 1569−1577.

(12) The surface disilane [═$SiH_2$] is present along with surface monosilane [≡SiH], depending on the transfer mechanism at hand during the formation of the surface hydrides. Spectroscopic indications suggest that they are not as affected as [≡SiH] in the reaction with ammonia. See: Rataboul, F.; Baudouin, A.; Thieuleux, C.; Veyre, L.; Coperet, C.; Thivolle-Cazat, J.; Basset, J.-M.; Lesage, A.; Emsley, L. *J. Am. Chem. Soc.* **2004**, *126*, 12541−12550.

(13) This elemental analysis also indicates that the coordination of a second molecule of ammonia on the tantalum center, [(≡$SiO)_2$Ta(═NH)($NH_2$)-($NH_3$)$_2$], **2·($NH_3$)$_2$** which could be possible, is on average not relevant under these reaction conditions.

(14) Mason, J. *Chem. Rev.* **1981**, *81*, 205−227.

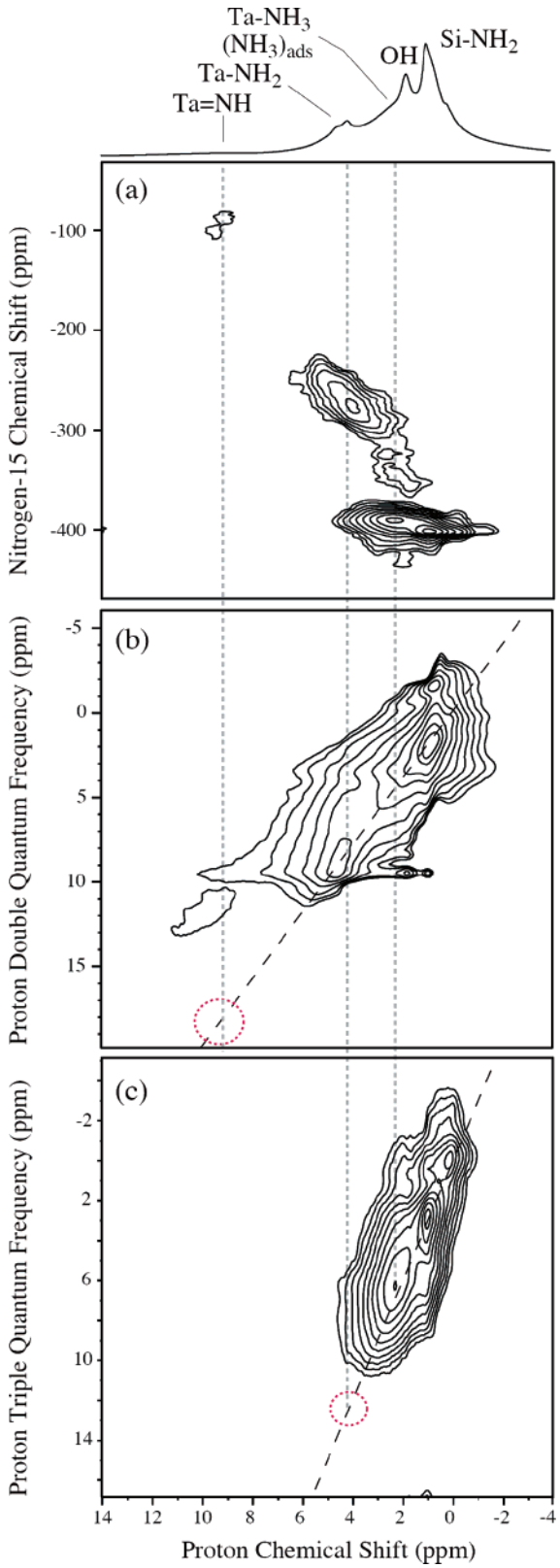


***Figure 2.*** (a) Two-dimensional $^{1}H-^{15}N$ HETCOR correlation spectrum of fully $^{15}N$-labeled complexes **2***, **2*·NH$_3$**, and [≡Si−$^{15}$NH$_2$] and comparison with two-dimensional double quantum (b) and triple quantum (c) correlation spectra. An exponential line broadening of 100 Hz was applied to all the proton dimensions before Fourier transform. The dotted gray lines correspond to the resonances of the tantalum NH, NH$_2$, and NH$_3$ protons. The dotted red circles underline the absence of autocorrelation peaks for the imido proton in the double quantum spectrum (b), and for the amido proton in the triple quantum spectrum (c). The experimental conditions are described in detail in the main text.

moiety, Ta(***N*H**$_2$). These chemical shifts are indeed located well within the expected spectral region for amido groups given the literature precedents on solution analogues: nitrogen-15 chemical shifts between −150 and −350 ppm have been reported for M(***N***HR) species, and proton chemical shifts between 3 and 7 ppm have been found for Ta$^{V}$(N***H***R) species.[15−17]

The identification of the imido and amido moieties of complex **2*** was further confirmed by 2D proton double quantum[18−22] and triple quantum NMR spectroscopy.[23−26] The 2D proton double-quantum (DQ) single-quantum (SQ) correlation spectrum of Figure 2b was recorded using the following general scheme: excitation of DQ coherences, $t_1$ evolution under proton homonuclear decoupling of double quantum coherences, reconversion of these coherences into observable magnetization, *Z*-filter, and detection. The corresponding 2D map yields ($\omega_1$,$\omega_2$) correlations between pairs of dipolar coupled (i.e., spatially close) protons. The DQ frequency in the indirect $\omega_1$ dimension corresponds to the sum of the two SQ frequencies of the two coupled protons and correlates in the $\omega_2$ dimension with the two individual proton resonances. Therefore, the observation of a DQ peak implies a close proximity between the two protons in question. Furthermore, two equivalent protons will give an autocorrelation peak located on the $\omega_1 = 2\omega_2$ line of the 2D map. Conversely, single spins will not give rise to diagonal peaks. In the same way, the proton TQ−SQ correlation spectrum of Figure 2c was recorded using the following scheme: excitation of TQ coherences (via a 90° proton pulse followed by a DQ excitation block), $t_1$ evolution under homonuclear decoupling of the TQ coherences, reconversion into observable magnetization, *Z*-filter, and detection. In analogy with the DQ−SQ correlation experiment, the TQ frequency in the $\omega_1$ dimension corresponds to the sum of the three SQ frequencies of the three coupled protons and correlates in the $\omega_2$ dimension with the three individual proton resonances. Three equivalent protons will give an autocorrelation peak along the $\omega_1 = 3\omega_2$ line of the 2D map. Conversely, groups of less than three equivalent spins will not give rise to diagonal signals in the spectrum. Two-dimensional DQ and TQ correlation experiments can thus be applied to determine in a reliable way the number of attached equivalent protons to a given X nucleus and thus to discriminate between the NH, NH$_2$, and NH$_3$ groups here.

In the DQ spectrum of Figure 2b, we clearly see that, as expected for a single attached proton, the Ta(N***H***) resonance of the imido moiety present in the proton spectrum at 9 ppm does not display an autocorrelation peak along the $\omega_1 = 2\omega_2$ line (red dotted circle). Conversely the two protons of the amido

(15) Bonanno, J. B.; Wolczanski, P. T.; Lobkovsky, E. B. *J. Am. Chem. Soc.* **1994**, *116*, 11159−11160.
(16) Burland, M. C.; Pontz, T. W.; Meyer, T. Y. *Organometallics* **2002**, *21*, 1933−1941.
(17) Royo, P.; Sanchez-Nieves, J. *J. Organomet. Chem.* **2000**, *597*, 61−68.
(18) Brown, S. P.; Spiess, H. W. *Chem. Rev.* **2001**, *101*, 4125−4156.
(19) Brown, S. P.; Schnell, I.; Brand, J. D.; Müllen, K.; Spiess, H. W. *J. Am. Chem. Soc.* **1999**, *121*, 6712−6718.
(20) Brown, S. P.; Lesage, A.; Elena, B.; Emsley, L. *J. Am. Chem. Soc.* **2004**, *126*, 13230−13231.
(21) Graf, R.; Demco, D. E.; Gottwald, J.; Hafner, S.; Spiess, H. W. *J. Chem. Phys.* **1997**, *106*, 885−895.
(22) Madhu, P. K.; Vinogradov, E.; Vega, S. *Chem. Phys. Lett.* **2004**, *394*, 423−428.
(23) Schnell, I.; Spiess, H. W. *J. Magn. Reson.* **2001**, *151*, 153−227.
(24) Schnell, I.; Lupulescu, A.; Hafner, S.; Demco, D. E.; Spiess, H. W. *J. Magn. Reson.* **1998**, *133*, 61−69.
(25) Shantz, D. F.; auf der Gunne, J. S.; Koller, H.; Lobo, R. F. *J. Am. Chem. Soc.* **2000**, *122*, 6659−6663.
(26) Friedrich, U.; Schnell, I.; Demco, D. E.; Spiess, H. W. *Chem. Phys. Lett.* **1998**, *285*, 49−58.

group, Ta(N***H***$_2$), give rise to a strong correlation at about (4.3 ppm, 8.6 ppm) in the DQ spectrum, whereas no autocorrelation peak (red dotted circle in Figure 2c) is observed in the TQ spectrum for this group at about (4.3 ppm, 12.9 ppm).

In the HETCOR spectrum, two nitrogen-15 resonances correlate with protons at around 2.2 ppm: a weak one at −340 ppm and a much more intense one at −390 ppm in the $^{15}$N dimension. They are assigned to two distinct $NH_3$ resonances: respectively the tantalum-coordinated ammonia, Ta(***N***H$_3$) of **2*·$^{15}$NH$_3$** and adsorbed ammonia. This is in agreement with literature data (the $^{15}$N chemical shift of ammonia adsorbed on zeolite 3 Å was reported at −386 ppm),[27] and we have also observed a peak at −385 ppm for MCM-41 exposed to $^{15}$N-ammonia (data not shown). The proton chemical shift for these $NH_3$ species, centered at around 2.2 ppm, is also in good agreement with literature precedents.[8] We also observed that the intensity of the adsorbed ammonia resonance at −390 ppm can be reduced by prolonged treatment of the sample under vacuum, whereas the intensity of the Ta(***N***H$_3$) resonance remains unaffected, indicating that the complex **2·NH$_3$** still coexists with **2** (data not shown). As expected for these three-proton moieties, an autocorrelation peak is clearly observed in the proton TQ spectrum (Figure 2c) at (2.2 ppm, 6.6 ppm).

A fifth correlation peak is observed in the 2D HETCOR spectrum (Figure 2a) at around (1 ppm, −400 ppm), which is assigned to the amido moiety of the silylamido species [≡Si−***N*****H**$_2$]. As expected, the corresponding proton resonance autocorrelates at (1 ppm, 2 ppm) in the DQ spectrum of Figure 2b. Note that an autocorrelation peak is also visible in the TQ spectrum. However, a drastic change in relative intensity is observed for the $NH_3$ and Si−$NH_2$ resonances in going from the 1D DQ to the TQ filtered proton spectra, with the TQ spectrum being significantly attenuated for the proposed Si−$NH_2$ group as compared to the $NH_3$ group (data not shown). The TQ correlation at (1 ppm, 3 ppm) is most likely due to residual alkyl groups formed on the surface during the synthesis of the starting hydrides **1a** and **1b** (see Experimental Section for further details) rather than to intermolecular correlations between the silylamido groups that are expected to be dispersed on the surface. The assignment of the [≡Si−$NH_2$] resonance was further confirmed by the independent synthesis of [≡Si−$^{15}NH_2$] on tantalum-free silica, obtained by reaction of $^{15}$N-labeled ammonia on silica dehydroxylated at 1000 °C (reaction 2). The addition of ammonia on silica, normally unable to induce N−H cleavage at room temperature,[28] becomes possible in this case due the drastic dehydroxylation treatment which produces few highly strained [≡SiOSi≡] bridges (0.15/nm$^2$), that undergo cleavage by bimolecular oxidative addition of otherwise unreactive bonds.[28−30]

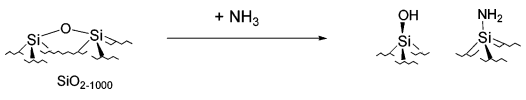

(2)

The solid-state $^{15}$N CPMAS NMR spectrum of the resulting [≡Si−$^{15}NH_2$] species shows two sharp signals at −385 and −400 ppm, assigned respectively to adsorbed ammonia and [≡Si−***N***H$_2$] groups (data not shown). Unlike the silylamido resonance, the resonance of adsorbed ammonia is affected by vacuum treatment.

Several off-diagonal DQ and TQ correlations, which are expected to result from a dipolar interaction between spatially adjacent nonequivalent protons, can be observed in b and c, respectively, of Figure 2. A DQ correlation is thus observed at about (9 ppm, 11 ppm) for the imido proton that can possibly result from a dipolar interaction with the adjacent protons of the coordinated or adsorbed ammonia (***N***H$_3$) that resonates at about 2.2 ppm. Similar DQ and TQ off-diagonal correlations can be observed for most of the other resonances most likely due to adsorbed ammonia, given the mobility of this species.

Finally, the proton resonance at 1.8 ppm corresponds to the unreacted [≡Si−O***H***] left over from the starting MCM-41 and that remaind unchanged throughout the syntheses (see Experimental Section for further details). As expected, this resonance does not yield any correlation in the $^1$H−$^{15}$N HETCOR spectrum. Similarly, no autocorrelation peak is observed in the DQ spectrum.

In summary, the combination of 2D HETCOR and proton DQ and TQ experiments allows for the complete unambiguous assignment of the $^1$H and $^{15}$N NMR spectra of complexes **2*** and **2*·$^{15}$NH$_3$** (Table 1). In particular DQ and TQ experiments were essential to discriminate between NH, $NH_2$, and $NH_3$ species bound to the tantalum and to therefore characterize unambiguously the surface organometallic complexes formed. Note that proton TQ experiments have been rarely used thus far to characterize solid systems and that this is the first application of this approach to surface complexes. Moreover, the implementation used here combines the indirect TQ evolution with state of the art homonuclear decoupling techniques to improve the spectral resolution in $\omega_1$, which is necessary for the characterization of real systems.

Finally, we note that the linewidths observed for the $^{15}$N resonances of the surface complexes (3000 Hz for the amido resonance at −270 ppm for example) reflect the presence of a certain degree of structural diversity among the surface species. (Individual $^{15}$N linewidths of less than 300 Hz were observed along the diagonal of nitrogen-15 proton-driven spin diffusion experiments, data not shown.) Conformational differences in the surface compounds are indeed expected with regard to the

***Table 1.*** $^1$H and $^{15}$N NMR Chemical Shifts of [(≡SiO)$_2$Ta(=$^{15}$NH)($^{15}NH_2$)], **2***, [(≡SiO)$_2$Ta(=$^{15}$NH)($^{15}NH_2$)($^{15}NH_3$)], **2*·$^{15}$NH$_3$**, [≡Si−$^{15}NH_2$], and Adsorbed $^{15}$N-Ammonia; All $^{15}$N Chemical Shifts Are Referenced with Respect to $CH_3NO_2$ at 0 ppm

| $^{15}$N NMR, δ/ppm | | $^1$H NMR, δ/ppm | |
|---|---|---|---|
| resonances | assignments | resonances | assignments |
| −87 | Ta=***N***H | 9.0 | Ta=N***H*** |
| −270 | Ta−***N***H$_2$ | 4.3 | Ta−N***H$_2$*** |
| −340 | Ta(***N***H$_3$) | 2.2 | Ta(N***H$_3$***) |
| −400[a] | Si−***N***H$_2$ | 1.0[a] | Si−N***H$_2$*** |
| −390[b,c] | adsorbed ***N***H$_3$ | 2.2[b,c] | adsorbed N***H$_3$*** |

[a] Observed also by reaction of highly dehydroxylated silica, $SiO_{2-1000}$, with $^{15}$N-ammonia that yields [≡Si−$^{15}NH_2$].[28,30] [b] Decreases under vacuum. [c] Observed also from exposure of pure MCM-41 to ammonia at room temperature, that yields adsorbed ammonia.[27] Assignments are in agreement with literature precedent.[27]

(27) Holland, G. P.; Cherry, B. R.; Alam, T. M. *J. Phys. Chem. B* **2004**, *108*, 16420−16426.
(28) (a) Morrow, B. A.; Cody, I. A.; Lee, L. S. M. *J. Phys. Chem.* **1975**, *79*, 2405−2408. (b) Morrow, B. A.; Cody, I. A. *J. Phys. Chem.* **1976**, *80*, 1998−2004.
(29) Scott, S. L.; Basset, J.-M. *J. Am. Chem. Soc.* **1994**, *116*, 12069−12070.
(30) Inaki, Y.; Kajita, Y.; Yoshida, H.; Ito, K.; Hattori, T. *Chem. Commun.* **2001**, 2358−2359.

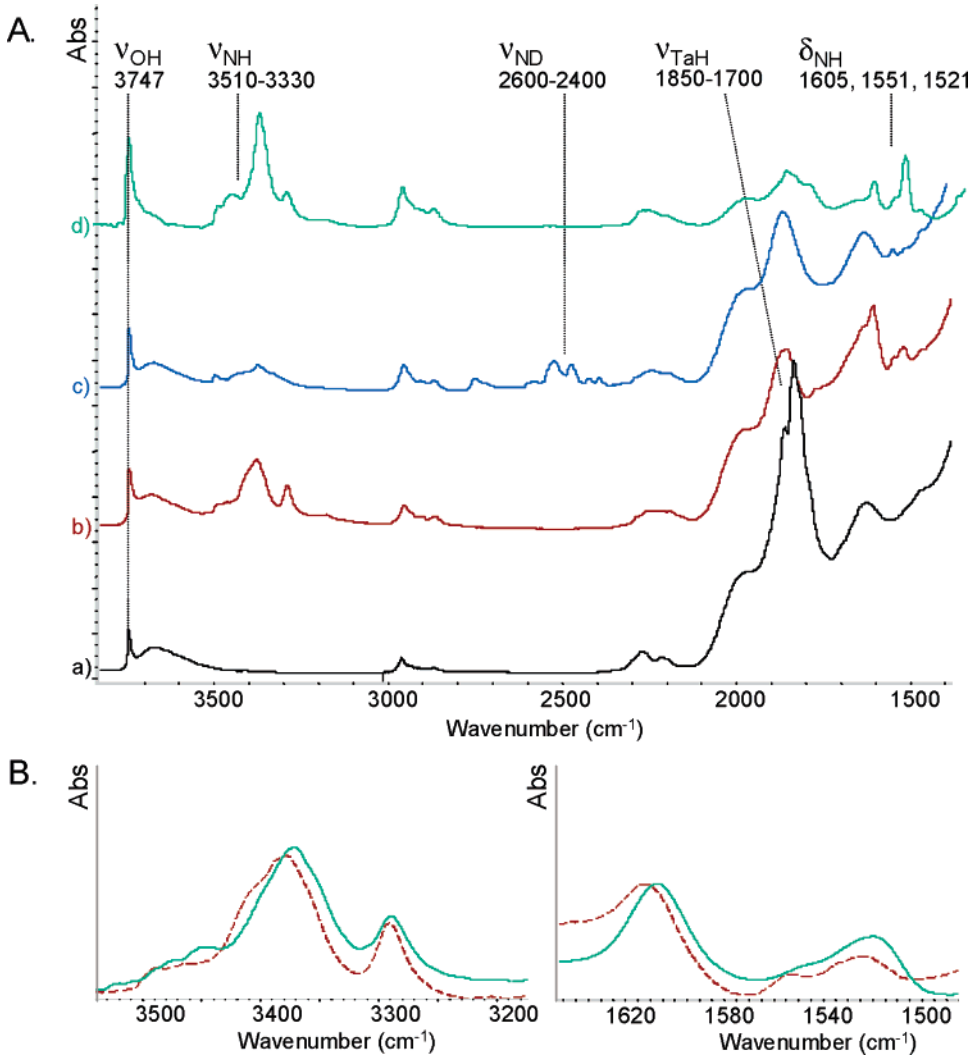


***Figure 3.*** (A) IR spectra of (a) starting MCM-41 silica-supported [(≡SiO)$_2$TaH], **1a**, and [(≡SiO)$_2$TaH$_3$], **1b**; (b) after addition to previous sample of $NH_3$ (40 Torr, 1 h, RT, followed by gas-phase evacuation); (c) after further addition of $D_2$ (500 Torr, 60 °C, 3 h); (d) after addition of $^{15}NH_3$ (17 Torr, RT, 1 h) to a new pellet of starting hydrides **1a** and **1b** prepared in a way similar to that for the sample used for spectrum a. (B) Enlarged portions of spectra b (dotted line) and d (solid line) zooming in the $\nu$(NH) [3550−3200 cm$^{-1}$] and $\delta$(NH) [1650−1500 cm$^{-1}$] regions.

known site heterogeneity of the starting surface hydrides[11] **1a** and **1b** and the coexistence of complexes **2** and **2·NH$_3$**.

The reaction of tantalum hydrides [(≡SiO)$_2$TaH], **1a**, and [(≡SiO)$_2$TaH$_3$], **1b**, with ammonia was also monitored by in situ infrared spectroscopy (Figure 3). In agreement with reaction 1, upon reaction of tantalum hydrides **1a** and **1b** with $NH_3$, the disappearance of $\nu$(TaH) stretching bands centered around 1830 cm$^{-1}$ was observed, with the concomitant appearance of vibration and deformation modes of N−H groups, centered around 3400 cm$^{-1}$. After 1 h at room temperature the reaction appeared complete. Addition of a large excess of $D_2$ to the reaction vessel induced H/D exchange (Figure 3c) to yield [(≡SiO)$_2$Ta(═ND)(ND$_2$)], **2-d**, its ammonia adduct **2-d·ND$_3$**, and [≡Si−ND$_2$]. The exchange reaction already occurred at room temperature and was accelerated by heating at 60 °C. The IR spectra of fully $^{15}$N-labeled compound obtained from the reaction of **1** and $^{15}NH_3$ were also collected (Figure 3d).

A comparative analysis of IR data of **2**, **2-d**, and **2*** and their ammonia adducts and the IR data of tantalum-free samples of adsorbed ammonia and [≡Si−NH$_2$] with respective isotopic analogues (data not shown) allowed the IR identification of the different $NH_x$ moiety frequencies (see Table 2). All the observed isotopic shifts are in good agreement with literature precedents for similar species[28,30,31] and with the expected isotopic frequencies based on the reduced-mass spring approximation.

An EXAFS study of surface species [(≡SiO)$_2$Ta(═NH)(NH$_2$)], **2**, and **2·NH$_3$** yielded spectra which can be satisfactorily fitted by a model based principally on a Ta(V) (bis)siloxy amido imido structure (see Figure 4). The best fit structure was obtained with one nitrogen atom at 1.79 Å, two oxygen atoms at 1.89 Å, and one nitrogen atom at 1.97 Å from the tantalum center (the results were similar with a $k^1$- instead of a $k^3$-weighting). These distances are in good agreement with values obtained from crystallographic data for molecular imido amido Ta(═N)(−O−)$_x$(−N<)$_y$ type complexes: 1.776(8) Å for Ta═N, 1.916 and 1.923(5) Å for Ta−O, and 1.951(7) Å for the Ta−N $\sigma$-bond in Ta(NAr)(OAr)$_2$(NArCH$_2$CH$_2$Ph),[32] 1.808(2) Å for Ta═N, 1.954(2) Å for Ta−O and 1.990(3) and 2.000(2) for the Ta−N $\sigma$-bonds in Ta(NAr)(OAr)($\kappa^3$-N$_2$NPy)[33]

(31) Gianotti, E.; Dellarocca, V.; Marchese, L.; Martra, G.; Coluccia, S.; Maschmeyer, T. *Phys. Chem. Chem. Phys.* **2002**, *4*, 6109−6115.
(32) Chamberlain, L. R.; Steffey, B. D.; Rothwell, I. P.; Huffman, J. C. *Polyhedron* **1989**, *8*, 341−349.
(33) Pugh, S. M.; Troesch, D. J. M.; Skinner, M. E. G.; Gade, L. H.; Mountford, P. *Organometallics* **2001**, *20*, 3531−3542.

***Table 2.*** Observed and Calculated[a] IR Frequencies ($cm^{-1}$) Upon Exposure of Silica-Supported Hydrides **1a** and **1b** to $NH_3$,[b] to $^{15}NH_3$,[b] and after H/D Exchange on the $^{14}N-$ Product[c] Yielding, Respectively: [(≡SiO)$_2$Ta(=NH)(NH$_2$)], **2**, [(≡SiO)$_2$Ta(=NH)(NH$_2$)(NH$_3$)], **2·NH$_3$**, and [≡Si−NH$_2$] (First Column); [(≡SiO)$_2$Ta(=$^{15}$NH)($^{15}$NH$_2$)], **2***, **2*·NH$_3$**, and [≡Si−$^{15}$NH$_2$] (Second Column), [(≡SiO)$_2$Ta(=ND)(ND$_2$)], **2-d**, **2-d·ND$_3$**, and [≡Si−ND$_2$] (Third Column); and Proposed Assignments (Fourth Column)

| $\nu$(NH$_x$) and $\delta$ (NH$_x$) from $NH_3$ observed | $\nu$($^{15}$NH$_x$) and $\delta$($^{15}$NH$_x$) from $^{15}NH_3$ observed (calculated)[a] | $\nu$(ND$_x$) and $\delta$ (ND$_x$) from $NH_3$ and $D_2$ observed (calculated)[a] | assignment |
|---|---|---|---|
| 3500 | 3490 (3492) | 2597 (2556) | $\nu_{NH}$ |
| 3462[d] | 3454 (3454 ) | 2578 (2528) | $\nu_{NH}$ |
| 3377 | 3372 (3369) | 2473 (2468) | $\nu_{NH}$ |
| 3293 | 3289 (3286) | 2422 (2405) | $\nu_{NH}$ ($NH_3$) |
| 1606 | 1602 (1602) | −[e] (1173)[f] | $\delta_{HNH}$ ($NH_3$) |
| 1550[d] | 1546 (1547) | −[e] (1132)[f] | $\delta_{HNH}$ (Si−NH$_2$) |
| 1521 | 1516 (1518) | −[e] (1110)[f] | $\delta_{HNH}$ (Ta−NH$_2$) |

[a] Calculated frequency using the spring approximation and the reduced mass theory for the moiety NH$_x$. [b] Obtained at room temperature after 1 h of reaction and removal of the gas phase. [c] Obtained by exposing the non-labeled sample to $D_2$ (570 Torr, 60 eq/Ta) at 60 °C for 3 h. [d]Similar frequencies at 3452 and 1552 $cm^{-1}$ were observed by reaction of highly dehydroxylated silica, $SiO_{2-1000}$, with $NH_3$. A further weak peak at 3530 was observed. Assignments to [≡Si−NH$_2$] in agreement with literature precedents.[28,30] [e] Not observed. [f] Predicted outside the available spectral window.

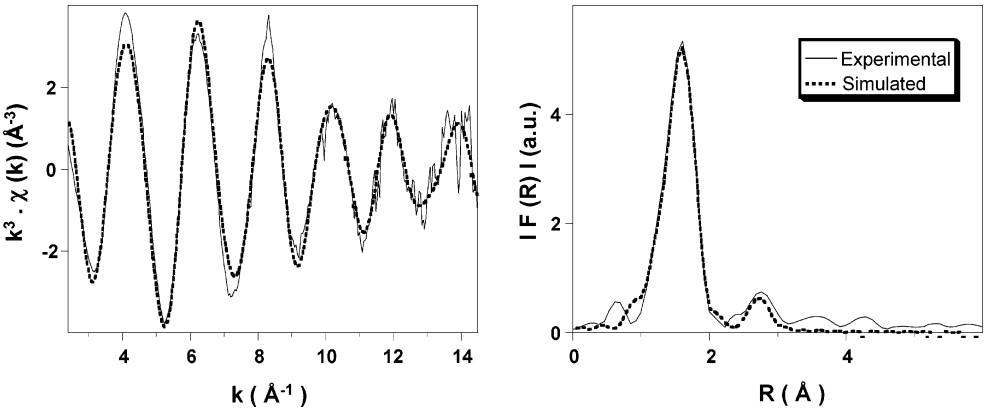


***Figure 4.*** Ta L$_{III}$-edge $k^3$-weighted EXAFS (left) and Fourier transforms (right) of the solid resulting from the reaction of $NH_3$ with [(≡SiO)$_2$TaH], **1a**, and [(≡SiO)$_2$TaH$_3$], **1b**, yielding [(≡SiO)$_2$Ta(=NH)(NH$_2$)], **2**, [(≡SiO)$_2$Ta(=NH)(NH$_2$)(NH$_3$)], **2·NH$_3$**, and [≡Si−NH$_2$]. Solid lines: experimental; dotted lines: spherical wave theory.

and fallwithin ranges usually observed for these distances: 1.70 to 1.83 Å for Ta=N and Ta ≡ N; 1.85 to 1.96 Å for Ta−O and 1.95 to 2.04 Å for Ta−N $\sigma$-bonds).[34] One additional shell was added to improve the fit: one nitrogen or oxygen at 3.03 Å, which may correspond to the nitrogen or oxygen atoms of [≡Si−NH$_2$] groups or siloxane bridges of the modified silica support. The inclusion of these extra parameters decreased the quality factor, $(\Delta\chi)^2/\nu$, from 1.67 ($\nu = 18$) for the three shells model to 1.57 ($\nu = 16$) for the four shells model. A fifth constrained shell was tentatively considered with ∼0.4 nitrogen at 2.30 Å, corresponding to a $\pi$-bonding nitrogen atom of $NH_3$ (this distance lies in the 2.20−2.60 Å Ta−N≡ range obtained for single crystals by XRD, e.g., 2.247(7) and 2.262(7) Å for the Ta−NH$_2$CHMe$_2$ distances in the tantalum imido amido amino complex Ta(N$^i$Pr)(NH$^i$Pr)(NH$_2$$^i$Pr)$_2$Cl$_2$,[37] 2.28(2) Å for Ta−NH$_2$CMe$_3$ in the tantalum imido amino complex [Ta(NCMe$_3$)($\mu$-OEt)Cl$_2$(NH$_2$CMe$_3$)]$_2$,[38] and 2.403(3) and 2.512(4) Å for Ta−N$^i$Pr< distances in ($^i$Pr$_2$-tacn)Cl$_2$Ta=NAr).[39] However, though the inclusion of this last shell improved the residue, it is not statistically validated by a decrease of the quality factor ($(\Delta\chi)^2/\nu = 1.61$ instead of 1.57) compared with the model with four shells, and this extra shell is thus not considered in Table 3. Simpler models (such as the one considering only two shells of light atoms, one for each of the two main peaks observed in the Fourier transform (right part of Figure 4)) led to worse fits with higher quality factors ($(\Delta\chi)^2/\nu > 2.6$ for the fit with only two shells). The EXAFS derived parameters are collected in Table 3.

***Table 3.*** Ta L$_{III}$-edge EXAFS-Derived Structural Parameters[a] ($k^3$ Weighting) of the Solid Resulting from the Reaction of $NH_3$ with [(≡SiO)$_2$TaH], **1a**, and [(≡SiO)$_2$TaH$_3$], **1b**, Yielding [(≡SiO)$_2$Ta(=NH)(NH$_2$)], **2**, [(≡SiO)$_2$Ta(=NH)(NH$_2$)(NH$_3$)], **2·NH$_3$**, and [≡Si−NH$_2$][b]

| scatterer | coordination number | distance from Ta (Å) | D.W. factor ($\sigma^2$, Å$^2$) |
|---|---|---|---|
| Ta=***N*** | 1 | 1.79(2) | 0.0023(14) |
| Ta−***O*** | 2 | 1.89(1) | 0.0023[c] |
| Ta−***N′*** | 1 | 1.98(2) | 0.0010(7) |
| Ta···***N″(O′)*** | 1 | 3.03(3) | 0.0025(15) |

[a] The values given in parentheses represent the errors generated in RoundMidnight. [b] Fit residue: $\rho = 5.6\%$ ($\Delta k = 2.4-14.6$ Å$^{-1}$, $\Delta R = 0.8-3.9$ Å); energy shift: $\Delta E_0 = 9 \pm 1$ eV, the same for all shells; overall scale factor: $S_0^2 = 0.96$; number of parameters fitted: $P = 8$; number of degrees of freedom in the fit: $\nu = 16$; quality factor of the fit: $(\Delta\chi)^2/\nu = 1.57$. [c] Shell constrained to a parameter above.

Upon exposure to water, the compound **2** and **2·NH$_3$** released some ammonia in the gas phase, as monitored by IR, and a substantial quantity of $NH_3$ remained adsorbed on the MCM-41 surface.

In summary, the combined use of in situ IR, EXAFS, and advanced solid-state NMR spectroscopy, coupled with chemical analyses (elemental analyses, titrations, hydrolysis), has therefore

(34) The Cambridge Structural Database: Allen, F. H. *Acta Crystallogr.* **2002**, *B58*, 380−388.
(35) Burland, M. C.; Meyer, T. Y.; Geib, S. J. *Acta Crystallogr. C* **2003**, *C59*, m46−m48.
(36) Bates, P. A.; Nielson, A. J.; Waters, J. M. *Polyhedron* **1985**, *4*, 1391−1401.
(37) Schmidt, J. A. R.; Chmura, S. A.; Arnold, J. *Organometallics* **2001**, *20*, 1062−1064.

*Scheme 1*

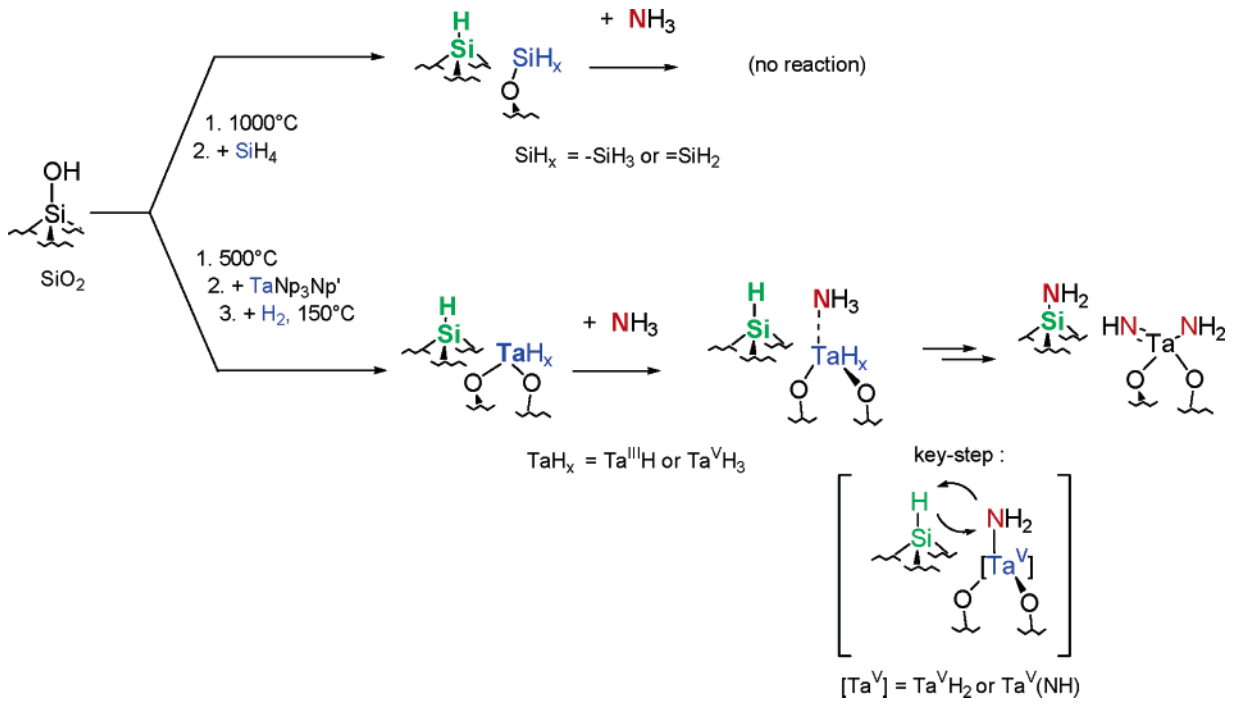


clearly shown that exposure to ammonia of the mesoporous silica-supported hydrides [(≡SiO)$_2$TaH], **1a**, and [(≡SiO)$_2$TaH$_3$], **1b**, leads to the complete conversion to Ta(V) amido imido species [(≡SiO)$_2$Ta(═NH)(NH$_2$)], **2**, and **2·NH$_3$**, and to the amination of some vicinal surface silicon hydrides to [≡Si−NH$_2$] with release of dihydrogen in the gas phase (see reaction 1). This system adds to the few previously reported well-defined organometallic complexes capable of cleaving N−H bonds of ammonia to yield either an amido[2,10] or an imido[9] complex. This first surface-organometallic system also displays an unprecedented stoichiometry, where both an imido and an amido species are formed on the same metal center. Surface Science studies on model catalysts for dinitrogen reduction to ammonia have also investigated the reaction of ammonia with metal surfaces.[38−41] High-resolution electron energy loss spectroscopy (HREELS) studies have clearly shown the formation of amido and imido surface species on several metal surfaces (such as, inter alia, Ru(11$\bar{2}$1),[39] Ni(110),[40] and Ru(0001)[41−43]), but no indication on the stoichiometry of the surface complexes thus obtained nor on other spectroscopic features of the metal imido and amido moieties is available.

**2.2. Tantalum-Assisted Formation of [≡Si−NH$_2$].** As discussed above, surface silylamido, [≡Si−NH$_2$], is obtained by addition of ammonia to the surface silanes [≡SiH][11,12] that are present in close proximity to [(≡SiO)$_2$TaH], **1a**, and [(≡SiO)$_2$TaH$_3$], **1b**. We have synthesized tantalum-free silica-supported silanes by reacting SiH$_4$ with highly dehydroxylated SiO$_{2-1000}$ (see reaction 3 for initial interaction between highly strained silica and SiH$_4$,[44] in analogy with reaction 2, vide supra):

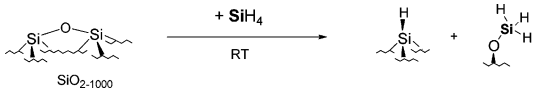


(3)

The surface silanes thus obtained do not react with ammonia at room temperature; in particular, the [≡SiH] present does not convert to [≡Si−NH$_2$] upon exposure to ammonia under the same experimental conditions described for reaction 1. The comparison between these two systems shows how tantalum is necessary to obtain the formation of the Si−N bond from unactivated ammonia (see Scheme 1). Such a Ta-assisted reactivity is well in line with the known reactivity of tantalum imido and amido with silanes[45] and suggests the interaction between products of reaction of the starting hydrides [(≡SiO)$_2$Ta$^{III}$H], **1a**, or [(≡SiO)$_2$Ta$^{V}$H$_3$], **1b**, with ammonia and the adjacent surface silanes [≡SiH] (see Scheme 1), although the precise mechanism remains to be elucidated. We note that the surface and/or chemical heterogeneity between [≡SiH] and [═SiH$_2$] present on the surface[12] can account for the observed partial reaction of the surface silanes.

In summary, the observed reaction of formation of silylamido [≡Si−NH$_2$] at room temperature is noteworthy, since it is a low-temperature and low-pressure fixation of a N$_1$ fragment from ammonia assisted by an adjacent isolated tantalum metal center. The reaction is thermodynamically driven by the strength of the Si−N bond; at the same time, the tantalum center is

(38) Nakata, T.; Matsushita, S. *J. Phys. Chem.* **1968**, *72*, 458−464. Many of the authors' assignments to $\nu$(NH) and $\nu$(NH$_2$) appear to overlap with our observation for adsorbed ammonia, thus shedding doubts on the authors' attributions.
(39) Dietrich, H.; Jacobi, K.; Ertl, G. *Surf. Sci.* **1996**, *352*−*354*, 138−141.
(40) Bassignana, I. C.; Wagemann, K.; Kueppers, J.; Ertl, G. *Surf. Sci.* **1986**, *175*, 22−44.
(41) Parmeter, J. E.; Wang, Y.; Mullins, C. B.; Weinberg, W. H. *J. Chem. Phys.* **1988**, *88*, 5225−5236.
(42) Rauscher, H.; Kostov, K. L.; Menzel, D. *Chem. Phys.* **1993**, *177*, 473−496.
(43) Shi, H.; Jacobi, K.; Ertl, G. *J. Chem. Phys.* **1995**, *102*, 1432−1439.
(44) The initial reaction between SiH$_4$ and the highly strained siloxy bridge is expected to be binuclear oxidative cleavage,[29,31] as reported in reaction 3. Further surface rearrangement of the silane hydrides to a mixture of [≡SiH] and [═SiH$_2$] is possible and is compatible with the observed experimental data (see Experimental Section). Minor formation of [≡SiOH], and hence presumably [≡Si−SiNH$_2$], is also observed.
(45) Gountchev, T. I.; Tilley, T. D. *J. Am. Chem. Soc.* **1997**, *119*, 12831−12841.

***Scheme 2.*** Proposed Elementary Steps for the Formation of Silica-Supported [(≡SiO)$_2$Ta(=NH)(NH$_2$)], **2**, and [(≡SiO)$_2$Ta(=NH)(NH$_2$)(NH$_3$)], **2·NH$_3$**, from Ammonia with Ta(III) Monohydride [(≡SiO)$_2$TaH], **1a**, and Ta(V) Trishydride [(≡SiO)$_2$TaH$_3$], **1b**

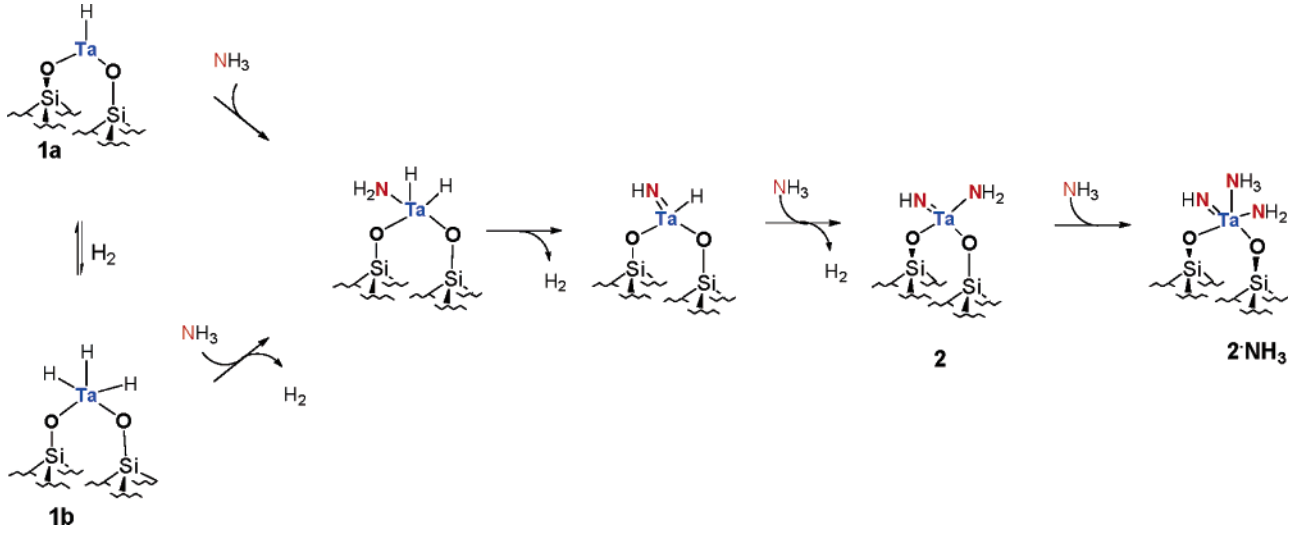


indispensable. This crucial role is most likely due to the unusual property of tantalum hydrides **1a** and **1b** (seldom encountered in organometallic chemistry[2,8−10]) of achieving N−H cleavage in ammonia at room temperature.

**2.3. Mechanistic Considerations on N−H Cleavage and Analogy with Methane C−H Activation.** The unusual reactivity of starting tantalum hydrides [(≡SiO)$_2$Ta$^{III}$H], **1a**, and [(≡SiO)$_2$Ta$^{V}$H$_3$], **1b**, toward ammonia to yield the amido/imido complex [(≡SiO)$_2$Ta(NH)(NH$_2$)], **2**, can be fully rationalized in terms of classical molecular organometallic elementary steps. Scheme 2 offers an example of elementary steps which rationalize the synthesis of the final product **2** from both the Ta(III) monohydride **1a** and the Ta(V) trishydride **1b**.

A precoordination of ammonia (not shown in the scheme) is expected to be involved.[46] Oxidative addition of the N−H bond on the Ta(III) centers, which is already reported in the literature[9,15] (or elimination of a hydride ligand as dihyrogen and formation of an amido on the Ta(V) center, which has been observed for other d$^0$ systems[10]) could readily account for the formation of the amido species. The successive transformation of the amido moiety into the imido species is expected to be a key step for the formation of **2**. The transformation of Ta(V)amidohydride in Ta(V)imido by 1,2-H$_2$ elimination, proposed in Scheme 2, has a very accurate molecular analogue in the complex ($^t$Bu$_3$SiO)$_3$Ta$^{V}$(H)(NH$_2$), which is thermally unstable and yields ($^t$Bu$_3$SiO)$_3$Ta$^{V}$(NH) by H$_2$ abstraction.[15] Furthermore, the general amido-to-imido reaction has several other molecular chemistry analogues,[4,5,9] and is typically rationalized as an α-H transfer from the amido to the metal to yield a metal−imidohydride complex.[5] Interesting analogies have been drawn between this amido-to-imido reaction and its methyl-to-methylidene analogue in organometallic molecular chemistry.[4,5] We extend here this analogy to surface organometallic chemistry, since a succession of α-H abstraction from [(≡SiO)$_2$Ta(CH$_3$)] to hydride methylidene [(≡SiO)$_2$Ta(H)(=CH$_2$)] and eventually to the methylidyne species [(≡SiO)$_2$Ta(≡CH)] has already been reported during the reaction of starting hydrides **1a** and **1b** with CH$_4$.[11,46]

(46) (a) Macgregor, S. A. *Organometallics* **2001**, *20*, 1860−1874. (b) Blomberg, M. R. A.; Siegbahn, P. E. M.; Svensson, M. *Inorg. Chem.* **1993**, *32*, 4218−4225.

## 3. Conclusion

We have shown that starting hydrides [(≡SiO)$_2$TaH], **1a**, and [(≡SiO)$_2$TaH$_3$], **1b**, cleave N−H bonds in ammonia to yield the new well-defined imido amido surface complex [(≡SiO)$_2$Ta(NH)(NH$_2$)], **2**, in equilibrium with its ammonia adduct **2·NH$_3$**. We have also shown that tantalum promotes the stoichiometric reaction of ammonia with surface silanes [≡Si−H] to give [≡Si−NH$_2$]. Notably, all the surface complexes thus obtained have been fully characterized with proton TQ solid-state NMR experiments, never before applied to surface science, that have allowed discrimination of NH, NH$_2$, and NH$_3$ groups in the surface complexes.

The solid-supported system adds to the very few literature reports[2,9,10] on systems capable of converting ammonia to well-defined imido or amido organometallic species. This gas/solid conversion of **1a** and **1b** to **2** and **2·NH$_3$** can be fully rationalized in terms of molecular organometallic elementary steps, indicating a central role played by α-H transfer reactions from Ta(NH$_x$) to Ta(NH$_{x-1}$) species. Such steps are known in solution organometallic chemistry, but were unprecedented in surface chemistry of isolated metal centers, thus contributing to reducing the cognitive gap between surface science and molecular organometallic chemistry.

Prior investigations in our laboratory had already shown that silica-supported tantalum hydrides **1a** and **1b** are able to activate C−H bonds in alkanes to form tantalum(V) alkyl, alkylidene, and alylidyne surface complexes.[11,48] This reactivity is tightly linked to the catalytic activity of **1a** and **1b** toward CH$_4$ and

(47) The analogy of the reaction of **1a** and **1b** with methane, that eventually leads to [(≡SiO)$_2$Ta(≡CH)],[11] suggests the possibility of [(≡SiO)$_2$Ta≡N] nitrido species occurring in the reaction with ammonia, if a further α-H reaction took place at the imido stage. Nevertheless, substantial presence of [(≡SiO)$_2$Ta≡N] would not be compatible with our observed experimental data. Furthermore, while methane activation requires higher temperatures (150 °C and above)[11] to obtain substantial conversion, the ammonia reaction with **1a** and **1b** occurs at room temperature. This low temperature is presumably too low to achieve nitridation of the surface, since TaN syntheses reported from Ta oxides and ammonia are performed at 350 °C or higher (see, for example: Lee, Y.; Nukumizu, K.; Watanabe, T.; Takata, T.; Hara, M.; Yoshimura, M.; Domen, K. *Chem. Lett.* **2006**, *35*, 352−353.).

(48) Vidal, V.; Theolier, A.; Thivolle-Cazat, J.; Basset, J.-M.; Corker, J. *J. Am. Chem. Soc.* **1996**, *118*, 4595−4602.

other alkanes for reactions such as H/D exchange,[49] hydrogenolysis,[50] metathesis,[51] and methane-olysis.[52] We have reported in this paper the first evidence of (surface)organometallic chemistry of metal imido and amido species from $NH_3$. It is thus conceivable that this advancement might be as fruitful for the emergence of N-based chemistry and catalysis from ammonia, as the discovery of the reactivity of **1a** and **1b** toward methane has been for the emergence of alkane-based catalytic reactions.[49−52]

## 4. Experimental Section

**General Procedure.** All experiments were carried out by using standard air-free methodology in an argon-filled Vacuum Atmospheres glovebox, on a Schlenk line, or in a Schlenk-type apparatus interfaced to a high-vacuum line ($10^{-5}$ Torr). [Ta($CH_2$$^t$Bu)$_3$(=CH$^t$Bu)] was prepared by the reaction of $TaCl_5$ with $^t$Bu-$CH_2MgCl$ according to literature procedure.[53] $^t$Bu-$CH_2MgCl$ was prepared from $^t$Bu-$CH_2Cl$ (98%, Aldrich, used as received) and Mg turnings (Lancaster).

MCM-41 mesoporous silica was supplied by the Laboratoire des Matériaux Minéraux, E.N.S. de Chimie Mulhouse, 3 rue Alfred Werner, 68093 Mulhouse Cedex, France. It was prepared according to literature method.[54] Its BET surface area, determined by nitrogen adsorption at 77 K, is 1060 $m^2/g$ with a mean pore diameter of 28 Å (BJH method). The wall thickness was found to be 14 Å by subtraction of the pore diameter from the unit cell parameter deduced from X-ray powder diffraction data.

MCM-41-supported [(≡SiO)Ta($CH_2$$^t$Bu)$_2$(=CH$^t$Bu)] was prepared by impregnation in pentane or by sublimation for in situ IR monitoring as previously reported.[11] Pentane was distilled on NaK alloy followed by degassing through freeze−pump−thaw cycles.

**Gas-phase analyses** of alkanes were performed on a Hewlett-Packard 5890 series II gas chromatograph equipped with a flame ionization detector and $Al_2O_3$/KCl on a fused silica column (50 m × 0.32 mm). Dihydrogen gas-phase analysis was performed on an Intersmat-IGC 120-MB gas chromatograph equipped with a catharometer.

**Infrared spectra** were recorded on a Nicolet 550-FT spectrometer by using an infrared cell equipped with $CaF_2$ windows, allowing in situ monitoring under controlled atmosphere. Typically 16 scans were accumulated for each spectrum (resolution, 2 $cm^{-1}$).

**Elemental analyses** were performed at the CNRS Central Analysis Service of Solaize, France, at the LSEO of Dijon, France, and at the Mikoanalytisches Labor Pascher in Remagen-Bandorf, Germany.

**NMR Spectroscopy.** All the NMR spectra were obtained on a Bruker 500 MHz wide-bore spectrometer using a double resonance 4-mm MAS probe. The samples were introduced under argon in a zirconia rotor, which was then tightly closed. The spinning frequency was set to 12.5 kHz for all the NMR experiments. The 1D $^{15}$N spectrum of Figure 1b was obtained from cross polarization (CP) from protons using an adiabatic ramped CP[55,56] to optimize the magnetization transfer efficiency. A proton radio frequency (RF) field of 50 kHz in the center of the tangential ramp was applied, while the RF field on nitrogen-15 was adjusted around the $\omega_{1H}-\omega_R$ matching condition.

The 2D proton−nitrogen-15 correlation spectrum of Figure 2a was recorded using a conventional solid-state heteronuclear correlation (HETCOR) experiment, which consists first in a 90° proton pulse, followed by a $t_1$ evolution period under a proton isotropic chemical shift and a CP step to transfer magnetization on the nitrogen-15 spins. The $^{15}$N signal is then recorded during $t_2$ under heteronuclear decoupling. During $t_1$, DUMBO-1 homonuclear decoupling[57] was applied, in order to average out the proton−proton dipolar couplings that leads to increased resolution in the proton dimension. A prepulse $\theta_1$ after $t_1$ ensures that the proton magnetization is flipped back from the tilted transverse plane (perpendicular to the effective field present under homonuclear decoupling) into the transverse ($x$,$y$) plane before the CP step, as described in reference.[58] For the spectrum of Figure 2a, a total of 113 $t_1$ increments of 64 $\mu$s with 256 scans each was recorded. The total experimental time was 18 h. The contact time was 1 ms, and the drepetition delay was 2 s. TPPM[59] heteronuclear decoupling (during $t_2$) and DUMBO-1 homonuclear decoupling (during $t_1$) were applied at RF fields of 100 kHz. An adiabatic ramped CP[55,56] was used with a proton RF field of 50 kHz in the center of the tangential ramp. Quadrature detection was achieved using the TPPI method[60] by incrementing the phase of the proton spin-lock pulse during the CP step. A scaling factor of 0.52 (as calibrated on model sample L-alanine) was applied to correct the proton chemical shift scale. Note that we found experimentally that homonuclear decoupling was required to observe all the correlations of the species bonded to the tantalum.

The 2D proton DQ−SQ correlation spectrum of Figure 2b was recorded according to the following general scheme: excitation of DQ coherences, $t_1$ evolution, reconversion into observable magnetization, $Z$-filter, and detection.[18−22,61] DQ excitation and reconversion were achieved using the POST-C7 pulse sequence.[62] A prepulse $\theta_1$ before $t_1$ ensures that there is no magnetization component along the effective field of the DUMBO decoupling sequence as described in reference 20. A second prepulse $\theta_1$ after $t_1$ rotates the magnetization back in preparation for the application of the DQ reconversion sequence. Proton magnetization was recorded during $t_2$ under MAS alone, while DUMBER-22 homonuclear decoupling[63] was applied during $t_1$ at a RF field of 100 kHz. The length of the POST-C7 excitation and reconversion block was set to 160 $\mu$s (corresponding to seven basic POST-C7 cycles). The phase dependence on the rotor phase of the POST-C7 sequence implies that there is a frequency shift of all peaks by $\omega_R$ from the centerband position in the DQ dimension.[64] The $\omega_1$ spectral width was chosen (10416 Hz) so that the DQ peaks were correctly folded in from their $\omega_R$-shifted frequencies. Quadrature detection in $\omega_1$ was achieved using the States-TPPI method.[65] A recycle delay of 1.5 s was used. A total of 80 $t_1$ increments of 96 $\mu$s with 384 scans each were recorded. The total experimental time for the DQ experiments was 12 h. A scaling factor of 0.56 was chosen (as calibrated on model sample L-alanine) to correct the DQ chemical shift scale. The efficiency of the DQ selection was about 40%.


(49) Lefort, L.; Coperet, C.; Taoufik, M.; Thivolle-Cazat, J.; Basset, J.-M. *Chem. Commun.* **2000**, 663−664.
(50) Chabanas, M.; Vidal, V.; Copéret, C.; Thivolle-Cazat, J.; Basset, J.-M. *Angew. Chem., Int. Ed.* **2000** *39*, 1962−1965.
(51) (a) Vidal, V.; Théolier, A.; Thivolle-Cazat, J.; Basset, J.-M. *Science* **1997**, *276*, 99−102. (b) Copéret, C.; Maury, O.; Thivolle-Cazat, J.; Basset, J.-M. *Angew. Chem., Int. Ed.* **1999**, *38*, 1952−1955.
(52) Soulivong, D.; Coperet, C.; Thivolle-Cazat, J.; Basset, J.-M.; Maunders, B. M.; Pardy, R. B. A.; Sunley, G. J. *Angew. Chem., Int. Ed.* **2004**, *43*, 5366−5369.
(53) Schrock, R. R.; Fellmann, J. D. *J. Am. Chem. Soc.* **1978**, *100*, 3359−3370.
(54) Chen, C. Y.; Li, H. X.; Davis, M. E. *Microporous Mater.* **1993**, *2*, 17−26.
(55) Hediger, S.; Meier, B. H.; Kurur, N. D.; Bodenhausen, G.; Ernst, R. R. *Chem. Phys. Lett.* **1994**, *223*, 283−288.
(56) Hediger, S.; Meier, B. H.; Ernst, R. R. *Chem. Phys. Lett.* **1995**, *240*, 449−456.
(57) Sakellariou, D.; Lesage, A.; Hodgkinson, P.; Emsley, L. *Chem. Phys. Lett.* **2000**, *319*, 253−260.
(58) Lesage, A.; Sakellariou, D.; Hediger, S.; Eléna, B.; Charmont, P.; Steuernagel, S.; Emsley, L. *J. Magn. Reson.* **2003**, *63*, 105−113.
(59) Bennett, A. E.; Rienstra, C. M.; Auger, M.; Lakshmi, K. V.; Griffin, R. G. *J. Chem. Phys.* **1995**, *103*, 6951.
(60) Marion, D.; Wüthrich, K. *Biochem. Biophys. Res. Commun.* **1983**, *113*, 967−974.
(61) Brown, S. P.; Zhu, X. X.; Saalwächter, K.; Spiess, H. W. *J. Am. Chem. Soc.* **2001**, *123*, 4275−4285.
(62) Hohwy, M.; Jakobsen, H. J.; Eden, M.; Levitt, M. H.; Nielsen, N. C. *J. Chem. Phys.* **1998**, *108*, 2686−2694.
(63) Elena, B.; de Paepe, G.; Emsley, L. *Chem. Phys. Lett.* **2004**, *398*, 532−538.
(64) Geen, H.; Titman, J. J.; Gottwald, J.; Spiess, H. *J. Magn. Reson., Ser. A* **1995**, *114*, 264−267.
(65) Marion, D.; Ikura, M.; Tschudin, R.; Bax, A. *J. Magn. Reson.* **1989**, *85*, 393−399.

The 2D proton TQ −SQ correlation spectrum of Figure 2c was recorded according to the following general scheme: excitation of TQ coherences, $t_1$ evolution, reconversion into observable magnetization, *Z*-filter, and detection.[23,24,26,66,67] TQ excitation was achieved by the sequential application of first a 90° proton pulse followed by a DQ POST-C7 pulse sequence as previously described in the literature.[25] As for the DQ−SQ correlation experiment a prepulse $\theta_1$ before $t_1$ ensures that there is no magnetization component along the effective field of the DUMBO decoupling sequence, whereas a second pulse $\theta_1$ after $t_1$ rotates the magnetization back in preparation for the application of the TQ reconversion sequence. A *Z*-filter is applied before direct detection of proton magnetization during $t_2$ under MAS alone. DUMBER-22 homonuclear decoupling[63] was applied during $t_1$ at a RF field of 100 kHz. The length of the POST-C7 excitation and reconversion block was set to 160 $\mu$s (corresponding to seven basic POST-C7 cycles). Quadrature detection in $\omega_1$ was achieved using the States-TPPI method.[65] A recycle delay of 1.5 s was used. A total of 128 $t_1$ increments of 32 $\mu$s with 288 scans each were recorded. The total experimental time for the TQ experiment was 15 h. A scaling factor of 0.56 was chosen to correct the TQ chemical shift scale. The efficiency for the TQ selection was about 4%. Both the DQ and the TQ experiments were first implemented on a model sample of L-alanine to ensure the correctness of the pulse programming. The pulse programs of all the NMR experiments presented in this paper are available upon request to the authors.

**Extended X-ray Absorption Fine Structure Spectroscopy (EXAFS).** The samples were packaged as pellets within an argon-filled dry box in double airtight sample holders equipped with Kapton windows. X-ray absorption spectra were acquired at the SRS of the CCLRC at Daresbury (UK) at beam-line 7.1 at room temperature at the tantalum $L^{III}$ edge with a double crystal Si(111) monochromator detuned 70% to reduce the higher harmonics of the beam. The energy calibration was carried out with a W foil. The spectra were recorded in the transmission mode between 9750 and 11000 eV. The spectra analyzed were the results of the averaging of three such acquisitions. It was carefully checked that the results obtained were comparable and reliable by comparing the first and last acquisition spectra and ensuring that no evolution could be detected. The data analyses were performed by standard procedures using the programs developed by Alain Michalowicz, in particular the EXAFS fitting program RoundMidnight2005.[68] In each spectrum the postedge background subtraction was carefully conducted using polynomial or cubic-spline fittings, and the removal of the low-frequency contributions was checked by further Fourier transform. Fitting of the spectrum was done on the $k^3$- and $k^1$-weighted data (a $k^3$-weighting is recommended when only light backscatterers with $Z < 36$ are present), using the following EXAFS equation where $S_0^2$ is a scale factor, $N_i$ is the coordination number of shell $i$, $r_c$ is the total central atom loss factor, $F_i$ is the EXAFS scattering function for atom $i$, $R_i$ is the distance to atom $i$ from the adsorbing atom, $\lambda$ is the photoelectron mean free path, $\sigma_i$ is the Debye−Waller factor, $\Phi_i$ is the EXAFS phase function for atom $i$, and $\Phi_c$ is the EXAFS phase function for the adsorbing atom:

$$\chi(k) \cong S_0^2 r_c(k) \sum_{i=1}^{n} \frac{N_i F_i(k,R_i)}{kR_i^2} \exp\left(\frac{-2R_i}{\lambda(k)}\right) \exp(-2\sigma_i^2 k^2) \sin[2kR_i + \Phi_i(k,R_i) + \Phi_c(k)]$$

The program FEFF8[69] was used to calculate theoretical values for $r_c$, $F_i$, $\lambda$, and $\Phi_i + \Phi_c$ based on model clusters of atoms. The refinements were performed by fitting the structural parameters $N_i$, $R_i$, $\sigma_i$, and the energy shift, $\Delta E_0$ (the same for all shells). The fit residue, $\rho$ (%), was calculated by the following formula:

$$\rho = \sum_k [k^3\chi_{exp}(k) - k^3\chi_{cal}(k)]^2 \sum_k [k^3\chi_{exp}(k)]^2 \times 100$$

As recommended by the Standards and Criteria Committee of the International XAFS Society,[70] an improvement of the fit took into account the number of fitted parameters. The number of statistically independent data points or maximum number of degrees of freedom in the signal, is defined as $N_{idp} = 2\Delta k \Delta R/\pi$. The $k^3$-weighted quality factor is defined as:

$$\frac{(\Delta\chi)^2}{\nu} = \frac{1}{\nu}\left(\frac{N_{idp}}{N_{pt}}\right)\left[\frac{\sum_k [k^3\chi_{exp}(k) - k^3\chi_{calc}(k)]^2}{\epsilon^2}\right]$$

where $\nu = (N_{idp} - P)$ is the number of degrees of freedom, $P$ is the number of parameters refined in the fit, $N_{pt}$ is the number of data points in the fitting range, and $\epsilon$ is the average statistical measurement error. This experimental error was evaluated with the smoothing method with a low-pass Fourier filtering, using the range above 7 Å in the *R* space. The inclusion of extra parameters were statistically validated by a decrease of the quality factor, $(\Delta\chi)^2/\nu$. The values of the statistical errors generated in RoundMidnight were multiplied by $[(\Delta\chi)^2/\nu]^{1/2}$ since the quality factors exceeded one, as recommended to take the systematic errors into account. The error bars thus calculated are given in parentheses after each refined parameter. The scale factor, $S_0^2$, was determined from the spectrum of $[Ta(=CH^tBu)(CH_2{}^tBu)_3]$[71] diluted in toluene, chosen as a reference (1C at 1.90 Å from the neopentylidene and 3C at 2.12 Å from the neopentyl ligands coordinated to tantalum). The value thus found for the scale factor $S_0^2 = 0.96$ was kept constant in all the fits.

**Hydrogenolysis of [(≡SiO)Ta($CH_2{}^tBu$)$_2$(=$CH^tBu$)]: Preparation of [(≡SiO)$_2$TaH], 1a, and [(≡SiO)$_2$TaH$_3$], 1b.** Loose orange powder of $[(\equiv SiO)_2Ta(=CH^tBu)(CH_2{}^tBu)_2]$ (400 mg, 0.26 mmol Ta) was treated twice at 150 °C with anhydrous hydrogen (550 Torr, 15 mmol, ~60 equiv/Ta) for 15 h. Gas chromatography analysis indicated the release of 13 ± 2 $CH_4$ resulting from the hydrogenolysis of 2,2-dimethylpropane, $CMe_4$ (2.6 ± 0.4 $CMe_4$/Ta, expected 3). The gas evolved during the reaction was removed under vacuum and the final hydrides [(≡SiO)TaH], **1a**, and [(≡SiO)$TaH_3$], **1b**, were recovered as a brown powder. As already reported,[11] some surface alkyl groups (<0.1 C/Ta) resist hydrogenolysis. Elemental Analysis: Ta 15.91%$_{wt}$, C 0.67%$_{wt.}$ Since such surface alkyls also resist all the further treatments with ammonia described below, no mention will be made of them except in the IR data below and in the discussion of the TQ $^1$H NMR spectrum in the main text. Likewise, some surface silanols from the starting MCM-41 do not undergo reaction with tantalum.[11] Since they remain unchanged throughout the syntheses with ammonia, they will not be further mentioned except in the IR data below and in the $^1$H NMR section of the main text.

For in situ IR studies, a typical preparation of starting hydrides **1a** and **1b** was the following: an excess of anhydrous dihydrogen (550 Torr, 7.5 mmol, 400 equiv per Ta) was added to an orange disk of $[(\equiv SiO)_2Ta(=CH^tBu)(CH_2{}^tBu)_2]$ (20−35 mg) prepared as previously described[11] and adjusted in a sample holder. The solid was heated at 150 °C for 15 h and the gas-phase removed after analysis.

IR spectra were recorded at each step of the preparation. Final IR: 3747 ($\nu_{OH}$), 3270−2850 ($\nu_{CH}$), 2270 ($\nu_{SiH}$), 2220 ($\nu_{SiH2}$), 2100−1600 ($\delta_{Si-O-Si}$), 1890−1700 ($\nu_{TaH}$), 1467 w, 1362 ($\delta_{CH}$) cm$^{-1}$.

(66) Carravetta, M.; auf der Gunne, J. S.; Levitt, M. H. *J. Magn. Reson.* **2003**, *162*, 443−453.
(67) Eden, M.; Levitt, M. H. *Chem. Phys. Lett.* **1998**, *293*, 173−179.
(68) Michalowicz, A. *Logiciels pour la chimie*; Société Française de Chimie: Paris, 1991; 102.
(69) Ankudinov, A. L.; Ravel, B.; Rehr, J. J.; Conradson, S. D. *Phys. Rev. B* **1998**, *58*, 7565−7576.
(70) *70. Reports of the Standards and Criteria Committee of the International XAFS Society*; http://ixs.iit.edu/subcommittee_reports/sc/, 2000.
(71) Fellmann, J. D.; Schrock, R. R.; Rupprecht, G. A. *J. Am. Chem. Soc.* **1981**, *103*, 5752−5758.

**Reaction of 1a and 1b with $NH_3$: Preparation of [(≡SiO)$_2$Ta(=NH)(NH$_2$)], 2, 2·$NH_3$, and [≡Si−NH$_2$].** An excess of anhydrous ammonia (40 Torr, 0.40 mmol, 5 equiv per Ta) was added to **1a** and **1b** (100 mg, 0.08 mmol Ta) and left at room temperature for 2 h and then was heated at 80 °C for 1 h. The gas phase was then removed under vacuum at 80° for 4 h. Gas phase analysis: 2 ± 1 $H_2$/Ta. Elemental Analysis Ta 6.42%$_{wt}$, N 1.33%$_{wt}$: 2.7 N/Ta. MAS $^1$H NMR: $\delta$ = 9.0 (Ta=N***H***), 4.3−4.0 (Si***H***, Si***H$_2$*** and Ta(N***H$_2$***)), 2.2 (TaN***H$_3$*** and MCM-41 adsorbed N***H$_3$***), 1.8 (SiO***H***), 1.0 (SiN***H$_2$***), 0.8 (C***H$_n$***).

**Reaction of 1a and 1b with $^{15}NH_3$: Preparation of [(≡SiO)$_2$Ta(=$^{15}$NH)($^{15}$NH$_2$)], 2*, 2*·$^{15}NH_3$, and [≡Si$^{15}$NH$_2$].** Addition of anhydrous $^{15}NH_3$ (30 Torr, 0.0 mmol, 3.6 equiv per Ta) to **1a** and **1b** (100 mg, 0.08 mmol Ta) was performed as described above. MAS $^1$H NMR $\delta$ = 9.0 (Ta=N***H***), 4.3−4.0 (Si***H***, Si***H$_2$*** and Ta−N***H$_2$***), 2.2 (TaN***H$_3$*** and MCM-41 adsorbed N***H$_3$***), 1.8 (SiO***H***), 1.0 (SiN***H$_2$***), 0.8 (C***H$_n$***). CP MAS $^{15}$N NMR $\delta$ = −87 (Ta=***N***H), −270 (Ta***N***H$_2$), −340 (Ta***N***H$_3$), −390 (MCM-41 adsorbed ***N***H$_3$), −400 (Si***N***H$_2$). Hetcor {$^{15}$N; $^1$H} NMR {−87; 9.0} (Ta=***NH***), {−270; 4.3} (Ta−***NH$_2$***), {−340; 2.2} (Ta***NH$_3$***), {−390; 2.2} (MCM-41 adsorbed NH$_3$), {−400; 1.0} (Si***NH$_2$***) ppm. $^1$H DQ NMR 4.3 (8.6 ppm in the $\omega_2$ dimension) (TaN***H$_2$***), 2.2 ± 1.0 ppm (4.5 ± 2.0 ppm in the $\omega_2$ dimension) (TaN***H$_3$*** and MCM-41 adsorbed N***H$_3$***), 1.0 ± 1.0 ppm (2.0 ± 2.0 ppm in the $\omega_2$ dimension) (SiN***H$_2$***, C***H$_n$***) ppm. $^1$H TQ NMR 2.3 (6.9 ppm in the $\omega_3$ dimension) (TaN***H$_3$*** and MCM-41 adsorbed N***H$_3$***), 0.1 (0.3 ppm in the $\omega_3$ dimension) (C***H$_n$***) ppm.

**In situ IR Study of $NH_3$ Addition to 1a and 1b.** An excess of $NH_3$ (3−10 Torr, 2−7 equiv) was added to a disk of the starting hydrides **1a** and **1b** (20 mg, 16 $\mu$mol Ta) at room temperature and allowed to react for 15 h. IR spectra were recorded after condensation of the gas phase in liquid dinitrogen through a cold finger. Elemental analysis: Ta 5.83%$_{wt}$, N 1.21%$_{wt}$: N/Ta = 2.7. Selected IR frequencies: 3500 ($\nu_{TaN-H}$), 3462 ($\nu_{=N-H}$), 3377 ($\nu_{TaN-H}$), 3293 ($\nu_{NH3}$), 1606 ($\delta_{NH3}$), 1550 ($\delta_{SiNH2}$), 1521 ($\delta_{TaNH2}$) cm$^{-1}$.

**IR Monitoring of the H/D Exchange on [(≡SiO)$_2$Ta(=NH)(NH$_2$)], 2, 2·$NH_3$ and [≡Si−NH$_2$].** A disk of **2**, **2·NH3**, and [≡Si−NH$_2$] was prepared as described above. The excess ammonia in the gas phase was removed under vacuum, and a large excess of deuterium (570 Torr, 60 equiv per tantalum) was added in the cell at room temperature overnight and heated at 60 °C for 3 h. Selected IR frequencies: 3502 ($\nu_{TaN-H}$), 3461 ($\nu_{=N-H}$), 3377 ($\nu_{TaN-H}$), 3290 ($\nu_{NH3}$), 2587 ($\nu_{ND}$), 2473 ($\nu_{ND}$), 2424 ($\nu_{ND}$), 2398 ($\nu_{ND3}$), 1605 ($\delta_{NH3}$), 1550 ($\delta_{SiNH2}$), 1520 ($\delta_{TaNH2}$) cm$^{-1}$.

**In situ IR Study of $^{15}NH_3$ Addition to 1a and 1b.** A small excess of 100% $^{15}$N-labeled ammonia (17 Torr, 12 equiv) was added to a disk of **1a** and **1b** (20 mg, 16 $\mu$mol Ta) at room temperature and allowed to react for 5 h. IR spectra were recorded when condensing the excess gas phase in a glass tube by liquid dinitrogen. Selected IR frequencies: 3490w ($\nu_{TaN-H}$), 3454w ($\nu_{=N-H}$), 3372w ($\nu_{TaN-H}$), 3289w ($\nu_{NH3}$), 1602w ($\delta_{NH3}$), 1546w ($\delta_{SiNH2}$), 1516w ($\delta_{TaNH2}$) cm$^{-1}$.

**Addition of $NH_3$ on Silica Dehydroxylated at 1000 °C: Formation of [≡Si−NH$_2$].** A disk of silica (34 mg) was dehydroxylated at 1000 °C for 15 h under vacuum to yield $SiO_{2-1000}$ (180 m$^2$/g, 0.15 bridges/100 Å$^2$).[29] $NH_3$ (300 Torr) was then added and heated at 500 °C for 15 h. The gas phase was removed under vacuum. Selected IR frequencies: 3530 ($\nu^{as}_{SiNH2}$), 3452 ($\nu^{sym}_{SiNH2}$), 1552 ($\delta_{SiNH2}$) cm$^{-1}$. Assignments were in agreement with previous reports.[28,30]

A similar synthesis was performed with $^{15}NH_3$, and after removal of the gas phase under vacuum, the NMR spectrum was collected. MAS $^{15}$N RMN: $\delta$ = −400 (Si$^{15}$***N***H$_2$) ppm.

**Addition of $SiH_4$ on Silica Dehydroxylated at 1000 °C.** A silica pellet (20 mg) was dehydroxylated 15 h at 500 °C and 15 h at 1000 °C under dynamic vacuum to yield $SiO_{2-1000}$. The disc was then contacted with 1 Torr of $SiH_4$ (13 $\mu$mol, 1300 equiv per strained siloxy bridges), by means of 200 Torr of a gas containing 0.5% of $SiH_4$ in Ar. The cell was heated up to 150 °C for 20 h. Selected IR frequencies: 2270 ($\nu_{SiH}$), 2220 ($\nu_{SiHx}$), 2100−1600 ($\delta_{Si-O-Si}$) cm$^{-1}$.

**Exposure of Surface Silanes to $NH_3$.** Ammonia (30 Torr, 30 equiv) was added to a pellet of surface silanes prepared as described above from $SiO_{2-1000}$ and $SiH_4$. After 72 h at room temperature, the cell was heated at 60 °C for 2 h. The gas phase was finally evacuated at room temperature under vacuum for 1 h. IR spectra before and after exposure to ammonia showed no substantial difference; in particular, no bands due to [≡Si−NH$_2$] were detected.

**Acknowledgment.** Insightful discussions with Richard R. Schrock are gratefully acknowledged. P.A. is grateful to the French Ministère délégué à la recherche for financial support. Some of the solid-state NMR spectra were recorded at the Rhône-Alpes European Large Scale Facility for NMR.

**Note Added after ASAP Publication.** Due to a production error, this paper was published ASAP on December 15, 2006, with a typographical error in the fourth sentence of the "Extended X-ray Absorption Fine Structure Spectroscopy (EXAFS)" part of the Experimental Section. The corrected version was published December 20, 2006.

JA0666809